Journal of Catalysis 277 (2011) 149–153

Contents lists available at ScienceDirect

Journal of Catalysis

journal homepage: www.elsevier.com/locate/jcat

Plasmonic enhancement of photocatalytic decomposition of methyl orange under visible light

Wenbo Hou [a], Zuwei Liu [b], Prathamesh Pavaskar [c], Wei Hsuan Hung [d], Stephen B. Cronin [a,b,c,*]

[a] Department of Chemistry, University of Southern California, Los Angeles, CA 90089, USA
[b] Department of Physics, University of Southern California, Los Angeles, CA 90089, USA
[c] Department of Electrical Engineering, University of Southern California, Los Angeles, CA 90089, USA
[d] Department of Materials Science, University of Southern California, Los Angeles, CA 90089, USA

ARTICLE INFO

Article history:
Received 7 September 2010
Revised 3 November 2010
Accepted 4 November 2010
Available online 18 December 2010

Keywords:
Plasmonic
Plasmon
Photocatalysis
Photocatalytic
Titanium dioxide
Gold nanoparticle

ABSTRACT

By integrating strongly plasmonic Au nanoparticles with strongly catalytic TiO_2, we observe enhanced photocatalytic decomposition of methyl orange under visible illumination. Irradiating Au nanoparticles at their plasmon resonance frequency creates intense electric fields, which can be used to increase electron–hole pair generation rate in semiconductors. As a result, the photocatalytic activity of large bandgap semiconductors, like TiO_2, can be extended into the visible region of the electromagnetic spectrum. Here, we report a 9-fold improvement in the photocatalytic decomposition rate of methyl orange driven by a photocatalyst consisting of strongly plasmonic Au nanoparticles deposited on top of strongly catalytic TiO_2. Finite-difference time-domain (FDTD) simulations indicate that the improvement in photocatalytic activity in the visible range can be attributed to the electric field enhancement near the metal nanoparticles. The intense local fields produced by the surface plasmons couple light efficiently to the surface of the TiO_2. This enhancement mechanism is particularly effective because of TiO_2's short exciton diffusion length, which would otherwise limit its photocatalytic efficiency. Our electromagnetic simulations of this process suggest that enhancement factors many times larger than this are possible if this mechanism can be optimized.

Published by Elsevier Inc.

1. Introduction

Photocatalytic decomposition of organic molecules has been of great interest for the removal of pollutants from water and air. Semiconductor photocatalysts (e.g., TiO_2, ZnO, SnO, In_2O_3) have been shown to effectively catalyze many chemical reactions, including the reduction of aqueous CO_2 [1–4], CO oxidation [5,6], water splitting [7–9], and the decomposition of pollutants [10–12]. While TiO_2 is one of the most promising photocatalysts for these purposes [12–14], it does not absorb light in the visible region of the electromagnetic spectrum. Because of TiO_2's short wavelength cutoff, there are very few solar photons (~4%) that can be used to drive this photocatalyst. Several attempts have been made to extend the cutoff wavelength of this catalyst, including doping [10,15,16] and defect creation [17,18]. However, these have only extended the absorption edge of TiO_2 to approximately 420 nm [10,15,16,19]. Therefore, most of the solar spectrum is still unable to drive this photocatalyst. Dye-sensitized solar cells have enabled the photovoltaic response of semiconductors to be extended to longer wavelengths by the direct transfer of charge from the dye molecules to the conduction band of the semiconductor [20]. The degradation of organic dye molecules has been studied under UV illumination of Au nanoparticle/TiO_2 composites previously by Falaras' and Kojima's groups [21–23]. The improvement in photocatalytic efficiency of TiO_2 with gold nanoparticles was attributed to high efficiency charge separation between the Au and TiO_2. In addition to photocatalytic enhancement under UV illumination, improved photocatalytic activity of Au nanoparticle/TiO_2 under visible irradiation has been also reported [24–26]. According to these previous works, a charge transfer mechanism occurs whereby the plasmon resonance excites electrons in Au, which are then transferred to the conduction band of the adjacent TiO_2. This proposed charge transfer mechanism is similar to that of a dye-sensitized solar cell [27]. However, the band energies for electrons and holes are very different for the metal–semiconductor interface, and no rigorous model for this process has been put forth in the context of plasmonics or catalysis [24]. Furthermore, the energy band alignment of anatase TiO_2 with respect to the work function of Au is energetically unfavorable for the direct transfer of electrons from Au to TiO_2.

Here, we demonstrate photocatalytic enhancement of TiO_2 under visible illumination by depositing Au nanoparticles on the TiO_2

* Corresponding author at: Department of Electrical Engineering, University of Southern California, Los Angeles, CA 90089, USA. Fax: +1 213 740 8677.
E-mail address: scronin@usc.edu (S.B. Cronin).

0021-9517/$ - see front matter Published by Elsevier Inc.
doi:10.1016/j.jcat.2010.11.001

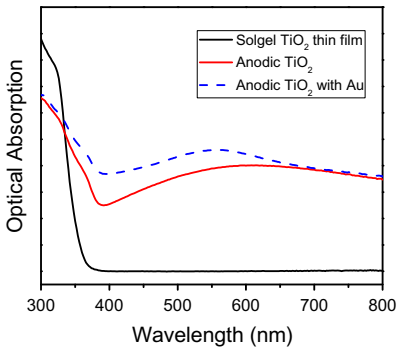

Fig. 1. UV–Vis absorption spectra of TiO_2 with and without gold nanoparticles.

surface. The enhancement can be accounted for based purely on the classical electric field enhancement near the Au nanoparticle surfaces. Finite-difference time-domain (FDTD) calculations of the electromagnetic response of the Au nanoparticles provide a quantitative prediction of the photocatalytic enhancement factor, which is in good agreement with our experimental values. This model is based on the near-field optical enhancement provided by the Au nanoparticles and does not require direct electron transfer between the materials. Several research groups have reported enhanced light absorption and/or photocurrents in solar cells using a similar plasmonic coupling mechanism. Here, we utilize the plasmonic field enhancement to improve TiO_2 photocatalysis in the visible wavelength range.

2. Experimental

TiO_2 was fabricated by the electrochemical oxidation of titanium foils using an ethylene glycol electrolyte containing 0.25 wt.% NH_4F at an anodization potential of 30 V [28]. The resulting material is commonly referred to as anodic titanium oxide (ATO). A gold film with a nominal thickness of 5 nm was then evaporated on the surface of the TiO_2. Evaporated Au thin films (~5 nm) are known to form island-like growth, which serve as good substrates for surface enhanced Raman spectroscopy (SERS) and other plasmonic phenomena [29,30]. Absorption spectra of the bare TiO_2 and Au nanoparticle/TiO_2 films were recorded on a Perkin–Elmer Lambda 950 UV/Vis/NIR with an integrating sphere detector. The photocatalytic activity was tested using methyl orange (MO) photodegradation as the model reaction. The decay in absorbance of the MO aqueous solution at 460 nm was monitored by Varian Cary 50 UV–Vis spectrophotometer after 1 h exposure to UV (365 nm, mercury lamp with a bandpass filter centered near 365 nm, 0.02 W) or green laser (532 nm, 0.2 W) irradiation.

3. Results and discussion

Fig. 1 shows the spherically integrated UV–Vis absorption spectra of TiO_2 with and without gold nanoparticles. The spectrum taken for an undoped TiO_2 film prepared by the solgel method (solid black curve) shows transparency for wavelengths above 370 nm, which corresponds to the bandgap of anatase TiO_2 [31,32]. However, the anodic TiO_2 film (red[1] solid curve) shows significant absorption at longer wavelengths due to N- and F-defects produced during the anodization process that create electronic states in the bandgap [19,33]. The absorption spectrum taken from anodic TiO_2 with gold nanoparticles (blue dashed curve) exhibits a peak in the

[1] For interpretation of color in Figs. 1–3, the reader is referred to the web version of this article.

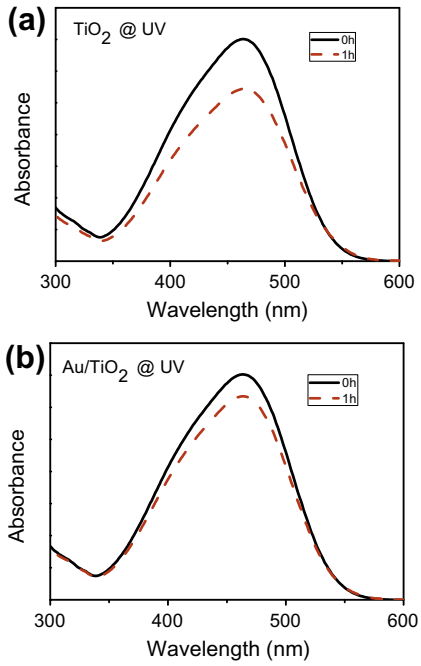

Fig. 2. UV–Vis spectra of MO aqueous solution before (black) and after (red) 1 h UV illumination using (a) TiO_2 and (b) Au nanoparticle/TiO_2 photocatalysts.

absorption around 546 nm, corresponding to the plasmon resonance of the Au nanoparticles, although the absorption of this film is quite broad due to its inhomogeneity [34].

Fig. 2 shows the photocatalytic degradation of MO achieved under UV irradiation. Here, the absorption spectra taken before and after irradiating with UV light (365 nm) are used to quantify the relative MO concentration and, hence, the photocatalytic decomposition rate. After 1 h of UV illumination, the absorbance of the MO aqueous solution, and hence concentration, is observed to drop by 23% for bare TiO_2 (Fig. 2a), but only by 10% for the Au nanoparticle/TiO_2 sample (Fig. 2b). Therefore, the addition of gold nanoparticles results in more than a 2-fold reduction in the photodecomposition rate due to the reduction in the active TiO_2 surface area. This reduction in active TiO_2 surface area can be seen in Fig. 4a, as the gold nanoparticle film covers a significant fraction of the TiO_2 surface, preventing it from coming into direct contact with the aqueous solution to be photocatalyzed. In this photochemical process, the photogenerated electrons and holes react with H_2O and O_2 in the MO aqueous solution to produce highly active oxidizing species, which in turn results in the photodecomposition of MO into inorganic final products (SO_4^{2-}, NO_3^-, NH_4^+, CO_2 and H_2O) [12,14,21,22,24].

Fig. 3 shows the MO absorption spectra taken before and after irradiating anodic TiO_2 with and without Au nanoparticles with visible light (532 nm laser). For bare TiO_2 (Fig. 3a), the absorbance (or concentration) of the MO solution is only observed to drop by 1.4% after 1 h of illumination. However, with the addition of gold nanoparticles, a 13% reduction in the MO absorbance is observed due to the plasmon-enhanced photocatalytic decomposition mechanism, as described below. This corresponds to a more than 9-fold enhancement in the photocatalytic activity. This 9-fold enhancement is not evident in the bulk optical absorption spectra in Fig. 1 because the improvement in photocatalytic activity is mainly due to the local near-field enhancement, which is not reflected in the bulk UV–Vis absorption spectra. In addition, the bulk UV–Vis spectra contain absorption processes that do not contribute to photocatalysis, such as recombination centers due to impurities.

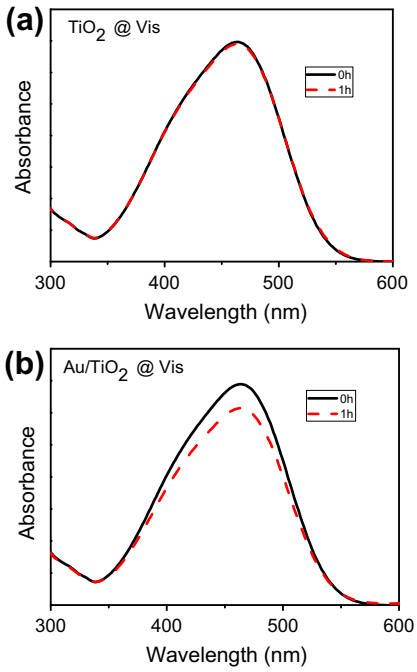

Fig. 3. UV–Vis spectra of MO aqueous solution before (black) and after (red) 1 h 532 nm laser illumination using (a) TiO_2 and (b) Au/TiO_2 as photocatalysts.

In order to understand the increase in photocatalytic activity under visible illumination (Fig. 3) and the reduction in photocatalytic activity under UV irradiation (Fig. 2) with the addition of Au nanoparticles, we perform FDTD numerical simulations of the electromagnetic response of these plasmonic/catalytic nanostructures [35]. Fig. 4a shows a scanning electron microscope (SEM) image of a gold nanoparticle-island film deposited on top of anodic TiO_2. In this SEM image, the light gray regions are gold nanoparticles, and the dark regions are in the interstitial space in between (underlying substrate alone). The electromagnetic response of these Au nanoparticle/TiO_2 composites is shown in Fig. 4b–d. The white lines in Fig. 4b and c outline the gold regions, based on the Au nanoparticle geometries from the SEM image in Fig. 4a. By comparing these figures, a one-to-one correspondence can be seen between the shapes traced out by the white lines in Fig. 4b and light gray regions in Fig. 4a. Local "hot spots" can be seen in regions between nearly touching Au nanoparticles. This is a well-known phenomenon, corroborated by the calculations of several research groups [36,37]. The importance of the local fields can be seen in Fig. 4d, which shows a cross-sectional plot of the electric fields in one of these hot spot regions. Here, the electric field intensity at the TiO_2 surface reaches 1000 times that of the incident electric field. Thus, the photoabsorption (and hence electron–hole pair generation) rate is 1000 times higher than that of the normal incident light. Furthermore, because this field is confined within a few nanometer of the TiO_2 surface, a majority of the plasmon-induced electron–hole pairs diffuse to the photocatalytic surface and contribute to the catalytic process. This is not the case for the normal, non-enhanced fields, which produce electron–holes pairs too far below the TiO_2 surface to contribute to photocatalysis.

Based on the results of the FDTD electromagnetic simulations shown in Fig. 4, we can calculate the expected photocatalytic enhancement due to this surface plasmon resonance phenomenon. Since the photon absorption rate is proportional to the electric field squared ($|E|^2$), integrated over the volume of the catalyst, the photocatalytic enhancement factor is given by

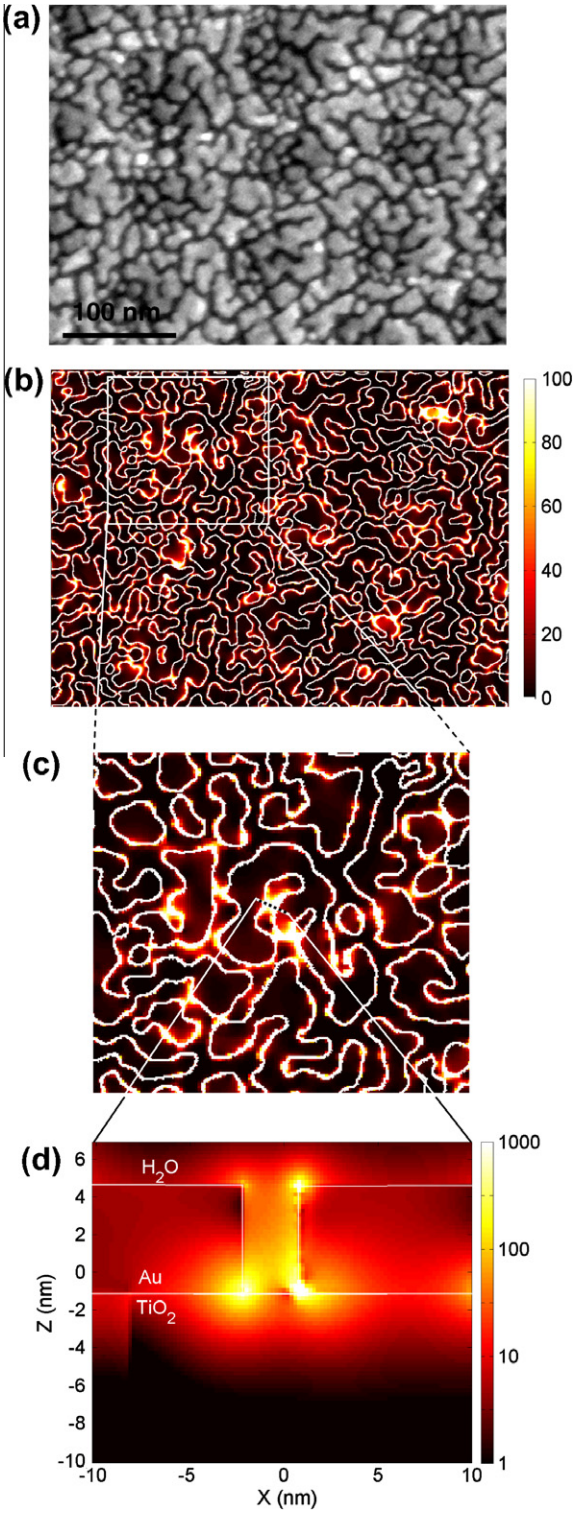

Fig. 4. (a) SEM image of a 5-nm thick Au island film deposited on anodic TiO_2. (b–d) Electric field intensities calculated at the interface of $Au–TiO_2$ using the FDTD method.

$$EF = \frac{\int_{-10\text{nm}}^{0} dz \int dxdy|E|^2}{\int_{-10\text{nm}}^{0} dz \int dxdy|E_0|^2}$$

Here, we integrate in z only from the TiO_2 surface ($z = 0$) to one exciton diffusion length below the surface ($z = -10$ nm). Performing this

integral over the whole area of the film that was simulated (400 nm × 300 nm) yields in an enhancement factor of 12X, which is close to the 9-fold enhancement observed experimentally. It should be noted, however, that this random distribution of Au nano-islands is far from optimized. If, instead, we only integrate over one individual "hot spot" region, as shown in Fig. 4c, the expected enhancement factor is 190X. Therefore, if the geometry of this plasmonic film could be optimized [38], enhancement factors many times larger than this could be achieved.

As can be seen from Fig. 4b, the electromagnetic response of the plasmonic film is dominated by a few localized hot spots. Therefore, a significant fraction of the plasmonic surface area is not utilized. In addition, chemically, there is a significant reduction in the TiO_2 surface area directly in contact with the aqueous solution, due to the presence of the Au nanoparticle film. Remarkably, we still observe a net improvement in the photocatalytic activity with the addition of Au nanoparticles, despite these two disadvantageous factors. The reason for this remarkably robust enhancement lies in the short exciton diffusion lengths of this anodic TiO_2. This enhancement relies on the presence of defect states in the TiO_2, which enable sub-bandgap absorption. The near-field optical enhancement provided by the Au nanoparticles is well-suited to this defect-rich material, which possess very short exciton diffusion lengths [39,40]. Therefore, virtually all of the photogenerated charge excited by these plasmon-enhanced fields contributes to the photocatalytic reaction. There is a trade-off, however, with doping. Doping (or defects) is needed in order to enable light absorption below the bandgap; however, these dopants result in very short exciton diffusion lengths, which ultimately spoil the photocatalytic performance. The plasmon enhancement mechanism that we have demonstrated here provides a way around this, by focusing light into the near-field at the TiO_2/photocatalytic surface, thus making it more robust to defects.

The photocatalytic activity of this Au nanoparticle/TiO_2 composite under UV (Fig. 2b) and visible (Fig. 3b) illumination is comparable. However, under UV illumination, the photon absorption mechanism is quite different from that under visible illumination. UV light is absorbed by direct interband transitions in the TiO_2 semiconductor. Under visible light, however, charge is excited to and/or from defect states in the bandgap of the TiO_2. Therefore, a direct comparison of UV and visible photocatalytic activity is not meaningful.

As a control experiment, we performed the photodegradation of MO aqueous solution under UV and green laser irradiation without any photocatalysts. Here, we observed no MO photodecomposition even after 24 h UV or green laser irradiation. Another control reaction was carried out by irradiating Au nanoparticles alone in solution without TiO_2. These Au nanoparticles were prepared according to the previous work of Hou et al. [41]. Even after 4 h of green laser irradiation with a power three times higher than those used in Fig. 3, no MO decomposition was observed. Thus, the presence of a semiconductor, such as TiO_2, is necessary in order to create electron–hole pairs, which drive the photodecomposition process. According to the previously proposed charge-transfer mechanism [26], visible light has enough energy to create electron–hole pairs on the Au surface capable of decomposing MO. However, if this were true, we would observe MO photodecomposition using only Au nanoparticles as the photocatalyst, which is not the case. The photocatalytic activity of the Au nanoparticle/TiO_2 photocatalyst was also tested under 633 nm and 785 nm laser illumination, which are below the plasmon resonance energy of Au nanoparticles. After 4 h illumination, no MO decomposition was observed. Therefore, in order for sufficient electric fields to be achieved, the laser energy must match the plasmon resonance frequency of the nanoparticles.

4. Conclusions

Summarily, we demonstrate plasmon resonant enhancement of the photocatalytic decomposition of methyl orange under visible light exposure by integrating strongly plasmonic Au nanoparticles with strongly catalytic TiO_2. While the plasmonic Au nanoparticles enhance the photocatalytic activity of TiO_2 in the visible range, they result in a reduction in the photocatalytic activity under UV exposure, due to the reduction in TiO_2 surface area exposed to the aqueous solution. Finite-difference time-domain simulations of these Au nanoparticle/TiO_2 photocatalysts show that the enhanced photocatalytic activity is due to the large plasmonic enhancement of the incident electromagnetic fields, which increases the electron–hole pair generation rate at the TiO_2 surface, and hence the photodecomposition rate of methyl orange. This enhancement mechanism relies on the presence of defect states in the TiO_2, which enables sub-bandgap absorption. The near-field optical enhancement of the Au nanoparticles couples light efficiently to the surface of the TiO_2, making its photocatalytic performance robust to defects.

Acknowledgments

This research was supported in part by AFOSR Award No. FA9550-08-1-0019, ARO Award No. W911NF-09-1-0240, and NSF Award No. CBET-0846725.

References

[1] T. Inoue, A. Fujishima, S. Konishi, K. Honda, Nature 277 (1979) 637–638.
[2] M. Halmann, M. Ulman, B. Aurianblajeni, Sol. Energy 31 (1983) 429–431.
[3] M. Anpo, H. Yamashita, Y. Ichihashi, S. Ehara, J. Electroanal. Chem. 396 (1995) 21–26.
[4] K. Adachi, K. Ohta, T. Mizuno, Sol. Energy 53 (1994) 187–190.
[5] J.C.S. Wu, T.H. Wu, T.C. Chu, H.J. Huang, D.P. Tsai, Top. Catal. 47 (2008) 131–136.
[6] W.X. Dai, X. Chen, X.X. Wang, P. Liu, D.Z. Li, G.S. Li, X.Z. Fu, Phys. Chem. Chem. Phys. 10 (2008) 3256–3262.
[7] T. Maschmeyer, M. Che, Angew. Chem. Int. Ed. 49 (2010) 1536–1539.
[8] O. Rosseler, M.V. Shankar, M.K.L. Du, L. Schmidlin, N. Keller, V. Keller, J. Catal. 269 (2010) 179–190.
[9] X.J. Sun, H. Liu, J.H. Dong, J.Z. Wei, Y. Zhang, Catal. Lett. 135 (2010) 219–225.
[10] X.H. Wang, J.G. Li, H. Kamiyama, Y. Moriyoshi, T. Ishigaki, J. Phys. Chem. B 110 (2006) 6804–6809.
[11] N. Kislov, J. Lahiri, H. Verma, D.Y. Goswami, E. Stefanakos, M. Batzill, Langmuir 25 (2009) 3310–3315.
[12] N. Talebian, M.R. Nilforoushan, Thin Solid Films 518 (2010) 2210–2215.
[13] Z.H. Wang, T.S. Jiang, Y.M. Du, K.M. Chen, H.B. Yin, Mater. Lett. 60 (2006) 2493–2496.
[14] C.H. Wu, J.M. Chern, Ind. Eng. Chem. Res. 45 (2006) 6450–6457.
[15] A.K.L. Sajjad, S. Shamaila, B.Z. Tian, F. Chen, J.L. Zhang, J. Hazard. Mater. 177 (2010) 781–791.
[16] S. Shamaila, A.K.L. Sajjad, F. Chen, J.L. Zhang, Appl. Catal. B: Environ. 94 (2010) 272–280.
[17] M. Takeuchi, H. Yamashita, M. Matsuoka, M. Anpo, T. Hirao, N. Itoh, N. Iwamoto, Catal. Lett. 67 (2000) 135–137.
[18] M. Takeuchi, H. Yamashita, M. Matsuoka, M. Anpo, T. Hirao, N. Itoh, N. Iwamoto, Catal. Lett. 66 (2000) 185–187.
[19] Y. Xie, X.J. Zhao, J. Mol. Catal. A: Chem. 285 (2008) 142–149.
[20] M. Gratzel, Nature 414 (2001) 338–344.
[21] I.M. Arabatzis, T. Stergiopoulos, D. Andreeva, S. Kitova, S.G. Neophytides, P. Falaras, J. Catal. 220 (2003) 127–135.
[22] C. Yogi, K. Kojima, T. Takai, N. Wada, J. Mater. Sci. 44 (2009) 821–827.
[23] C. Yogi, K. Kojima, N. Wada, H. Tokumoto, T. Takai, T. Mizoguchi, H. Tamiaki, Thin Solid Films 516 (2008) 5881–5884.
[24] E. Kowalska, O.O.P. Mahaney, R. Abe, B. Ohtani, Phys. Chem. Chem. Phys. 12 (2010) 2344–2355.
[25] Y. Tian, T. Tatsuma, Chem. Commun. (2004) 1810–1811.
[26] Y. Tian, T. Tatsuma, J. Am. Chem. Soc. 127 (2005) 7632–7637.
[27] B. O'Regan, M. Grätzel, Nature 353 (1991) 737.
[28] C.A. Grimes, J. Mater. Chem. 17 (2007) 1451–1457.
[29] R. Kumar, H. Zhou, S.B. Cronin, Appl. Phys. Lett. 91 (2007) 223105-1–223105-3.
[30] R.P. Vanduyne, J.C. Hulteen, D.A. Treichel, J. Chem. Phys. 99 (1993) 2101–2115.
[31] N. Serpone, D. Lawless, R. Khairutdinov, J. Phys. Chem. 99 (1995) 16646–16654.
[32] A. Bendavid, P.J. Martin, A. Jamting, H. Takikawa, Thin Solid Films 355 (1999) 6–11.

[33] Q. Li, J.K. Shang, Environ. Sci. Technol. 43 (2009) 8923–8929.
[34] I. Doron-Mor, Z. Barkay, N. Filip-Granit, A. Vaskevich, I. Rubinstein, Chem. Mater. 16 (2004) 3476–3483.
[35] A. Taflove, S.C. Hagness, Computational Electrodynamics: The Finite-Difference Time-Domain Method, vol. xxii, Artech House, Boston, 2005.
[36] F. Le, D.W. Brandl, Y.A. Urzhumov, H. Wang, J. Kundu, N.J. Halas, J. Aizpurua, P. Nordlander, ACS Nano 2 (2008) 707–718.
[37] S.L. Zou, G.C. Schatz, Chem. Phys. Lett. 403 (2005) 62–67.
[38] P. Pavaskar, S.B. Cronin, Appl. Phys. Lett. 94 (2009) 760818-1–760818-10.
[39] K.S. Liu, H.G. Fu, K.Y. Shi, F.S. Xiao, L.Q. Jing, B.F. Xin, J. Phys. Chem. B 109 (2005) 18719–18722.
[40] B. Smarsly, D. Grosso, T. Brezesinski, N. Pinna, C. Boissiere, M. Antonietti, C. Sanchez, Chem. Mater. 16 (2004) 2948–2952.
[41] W.B. Hou, N.A. Dehm, R.W.J. Scott, J. Catal. 253 (2008) 22–27.